DOI: http://dx.doi.org/10.22104/jpst.2015.65

Journal of Particle Science and Technology (2015) 13-19

Journal of Particle Science and Technology

J | P | S | T

jpst.irost.ir

Kinetic Modeling of the High Temperature Water Gas Shift Reaction on a Novel Fe-Cr Nanocatalyst by Using Various Kinetic Mechanisms

Seyed Mahdi Latifi*, Mohammad Amin Ghotbi Ravandi

Department of Chemical Technologies, Iranian Research Organization for Science and Technology (IROST), Tehran, Iran

HIGHLIGHTS

- The kinetic data for high temperature water gas shift reaction on a novel Fe-Cr and a commercial Fe-Cr-Cu catalysts were collected
- The kinetic of the catalysts was modeled by using redox, associative-based models and an empirical one
- The dependence of the reaction rate on the concentration of CO was found to be greater than that of H_2O
- The novel catalyst showed more activation energy reducing than the commercial one

GRAPHICAL ABSTRACT

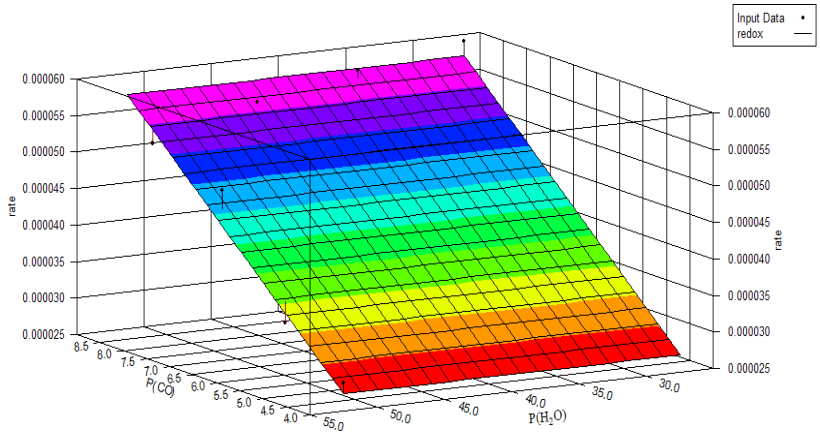

ARTICLE INFO

Article history:
Received 28 Septamber 2014
Received in revised from
8 November 2014
Accepted 8 November 2014

Keywords:
water gas shift reaction
Fe-Cr nanocatalyst
kinetic modeling
associative and
redox mechanisms
activation energy

ABSTRACT

In this work the kinetic data demanded for kinetic modeling were obtained in temperatures 350, 400, 450 and 500 °C by conducting experimentations on a Fe-Cr nanocatalyst prepared from a novel method and a commercial Fe-Cr-Cu one. The collected data were subjected to kinetic modeling by using two models derived from redox and associative mechanisms as well as an empirical one. The coefficients obtained for H_2O reduction to H_2 was much higher than those resulted for CO oxidation to CO_2. In addition, the rate of H_2O adsorption was shown to be greater than that of the CO adsorption on the catalyst surface in various temperatures. The activation energy of the novel catalyst calculated from the empirical model constants was lower than that of the commercial one.

* *Corresponding author Tel: +98 21 56276624*
E-mail address: latifi@irost.ir

1. Introduction

Water gas shift reaction (WGSR) expressed by [1]

$$CO(g) + H_2O(g) \rightleftharpoons CO_2(g) + H_2(g) \quad (1)$$

$$\Delta H^0_{298} = -41.09 \text{ kJ / mol}$$

is one of the prominent industrial reactions used in several chemical process and technologies as ammonia production and fuel cells. Because of thermodynamic limitations, the reaction is conducted in two sequential steps i.e. high temperature step (HTS), which occurs in 300 to 500 °C and low temperature step (LTS), which progresses in 300-450 °C temperature range. It is noteworthy to say that various catalysts have been introduced for conducting shift reactions [2,3] but in industrial uses, LTS and HTS are mainly catalyzed by Cu- and Fe-based catalysts, respectively [4].

It is obvious that the reaction rate is one of the most essential data has to be collected for reactor design and is usually predicted by those kinetic models that fitted well the reaction data. Therefore, modeling the kinetic behavior of the water gas shift reaction has received the attention of several researches [5,6]. The reaction kinetic can be studied from the views of the elementary steps involved in the reaction, called microkinetic method, and the empirical approaches. The WGSR has been studied through microkinetic approach by using regenerative and associative mechanisms. Regenerative mechanism (also known as redox mechanism) includes an oxidation- reduction cycle, occurring on the catalyst surface as follows [5].

$$H_2O + \text{red} \rightarrow H_2 + \text{ox} \quad (2)$$

$$CO + \text{ox} \rightarrow CO_2 + \text{red} \quad (3)$$

Surveying literature shows that both high and low temperature water gas shift reactions have been explained by redox mechanism [5]. Both forward and reverse WGSR were studied by using redox mechanism at low temperatures [7]. Redox mechanism including eight step elementary reactions bas been taken into account for low temperature WGSR on copper catalyst [8]. By using density functional method and slab models, it was shown that WGSR over Cu catalyst conformed redox mechanisms [9].

In associative mechanism, adsorbed reactants interact to form an adsorbed intermediate, which converts to H_2 and CO_2 after decomposition.The Langmuir-Hinshelwood model, which represents the associative mechanism, is expressed by [5] .

$$CO(g) \rightarrow CO(ads) \quad (4)$$

$$H_2O(g) \rightarrow H_2O(ads) \quad (5)$$

$$CO(ads) + H_2O(ads) \rightarrow [*] \rightarrow CO_2(ads) + H_2(ads) \quad (6)$$

$$CO_2(ads) \rightarrow CO_2(g) \quad (7)$$

$$H_2(ads) \rightarrow H_2(g) \quad (8)$$

Some authors considered formic acid [10] and carboxyl [11] as the intermediate and assumed possible pathways for them to decompose to reactants and products. It has been reported that compared to formate mechanism, carboxyl one was more probable mechanism for WGSR on Cu [12] and Pt [13] catalysts. Some works on water gas shift mechanism over several metal catalysts revealed that the Langmuir Hinshelwood model fitted well with kinetic data [14]. Stationary and transient studies on high temperature WGSR by using associative mechanisms indicated that the CO adsorption, CO_2 desorption and H_2 formation were controlling steps for reaction rate [15]. Also in some researches, the associative and redox mechanisms were found to be the dominant mechanisms in low and high temperature ranges, respectively [16].

Reviewing the works done on the WGSR kinetics reveals the fact that low temperature WGSR has greater share of the reported researches. In addition, it can be found that depending on the used catalyst, various kinetic models have this capability to predict the reaction kinetic behavior. In this work, we aimed at studying the kinetic of high temperature WGSR on a Fe-Cr nanocatalyst prepared by a novel method and a commercial one by conducting experimentation and then modeling the obtained results by two models derived from redox and associative mechanisms and an empirical-based model.

2. Experimental

2.1. Catalyst Samples

The novel Fe-Cr nanocatalyst was fabricated by thermolysis of the $[Fe(H_2O)_6][Cr(C_2O_4)_3].4H_2O$ and its detailed preparation procedure is mentioned elsewhere [17].The commercial catalyst sample for high temperature WGSR was provided from Sudchemie. The characteristics of the novel catalysts are presented in Table 1.

Table 1.
Novel catalyst characteristics.

BET surface area (m^2/g)	Crystallite size (nm)
118.4	13

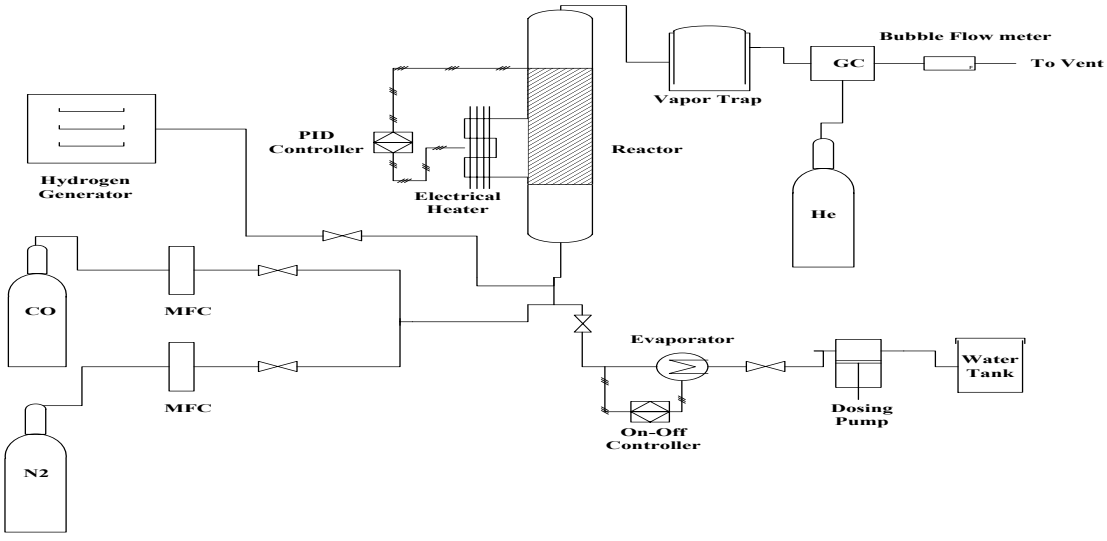

Fig. 1. Experimental setup for collecting kinetic data.

Table 2.
Kinetic data for the commercial catalyst.

	T(K)	P_{CO}(kpa)	P_{H2o}(kpa)	P_{N2}	$r_{CO} \times 10^{-5}$ [CO mol/(g_{cat}.s)]
Serie1	623	8.01	53.20	40.08	4.06
		8.28	44.68	48.33	4.31
		8.35	37.25	55.69	4.44
		8.49	29.07	63.73	4.62
	673	8.31	51.40	41.58	5.76
		8.42	43.70	49.17	6.12
		8.48	36.25	56.56	6.41
		8.72	27.14	65.43	6.99
	723	7.61	55.60	38.08	7.05
		8.53	43.00	49.77	10.60
		8.57	35.57	57.16	11.20
		8.67	27.54	65.08	11.40
	773	8.24	51.83	41.23	13.10
		8.42	43.70	49.17	15.60
		8.54	35.80	56.95	16.50
		8.72	27.14	65.43	17.30
Serie2	623	8.01	53.20	40.08	4.06
		8.28	44.68	48.33	4.31
		8.35	37.25	55.69	4.44
		8.49	29.07	63.73	4.62
	673	8.31	51.40	41.58	5.76
		8.42	43.70	49.17	6.12
		8.48	36.25	56.56	6.41
		8.72	27.14	65.43	6.99
	723	7.61	55.60	38.08	7.05
		8.53	43.00	49.77	10.60
		8.57	35.57	57.16	11.20
		8.67	27.54	65.08	11.40
	773	8.24	51.83	41.23	13.10
		8.42	43.70	49.17	15.60
		8.54	35.80	56.95	16.50
		8.72	27.14	65.43	17.30

2.2 Experimental Setup

For collecting the experimental data demanded for kinetic modeling, a reactor system that included a thermowell-equipped stainless steel tube (ID=2mm) was used. Heat power was supplied from an electrical heater that coiled around the outer surface of the tube and the temperature of the reactor was controlled by using a PID controller. The flow rates of CO and N_2 were controlled and measured by means of mass flow controllers (MFCs). For each run 0.2 gr of catalyst sample (mesh 25-35) was weighted and then put between layers of inert material. De-ionized water was sent to a vaporizer (400 K) by using a dosing pump (Milton Roy, Model CEP133-392S3) and then directed to the reactor. Before entering the reaction zone, by passing through a quartz granules packed bed, gas streams and vapor mixed completely. To analyze the CO content, the product stream after passing through a condenser was sent to an on-line gas chromatograph (molecular sieve 5A 80/100). It should be noted that before any run, the catalyst samples were reduced at 350 ^oC for 3 h in a hydrogen/nitrogen mixture (50% vol. H_2).

3. Results and Discussion

3.1. Kinetic data collecting

The kinetic data obtained from experimentations are presented in Table 2 and Table 3.

Table 3.
Kinetic data for the novel catalyst.

	T(K)	P_{CO}(kpa)	P_{H2O}(kpa)	P_{N2}	$r_{co}\times10^{-5}$ [CO mol/(g_{cat}.s)]
Serie1	623	4.04	52.78	44.48	1.07
		5.41	52.54	43.35	1.77
		6.72	52.86	41.72	2.33
		8.08	52.78	40.44	2.90
	673	4.16	51.29	45.85	1.46
		5.56	51.21	44.53	1.80
		6.95	51.21	43.14	2.16
		8.34	51.21	41.75	3.08
	723	4.09	52.21	45.00	2.86
		5.52	51.55	44.23	3.35
		6.93	51.38	42.99	4.85
		8.17	52.21	40.92	5.25
	773	4.14	51.55	45.61	5.31
		5.48	51.96	43.86	7.22
		6.71	52.94	41.65	7.81
		8.09	52.70	40.51	9.00
Serie2	623	8.29	51.55	41.46	1.60
		8.50	43.18	49.62	1.83
		8.65	34.97	57.68	2.05
		8.77	26.73	65.80	2.18
	673	8.34	51.21	41.75	2.21
		8.43	43.68	49.19	2.30
		8.57	35.55	57.18	2.54
		8.72	27.13	65.45	2.66
	723	8.18	52.21	40.91	5.24
		8.46	43.48	49.36	5.55
		8.57	35.55	57.18	5.80
		8.72	27.13	65.45	5.98
	773	8.10	52.70	40.50	8.41
		8.50	43.18	49.62	8.50
		8.63	35.08	57.59	8.55
		8.80	26.46	66.04	8.60

3.2. Kinetic modeling

3.2.1. Redox mechanism

The first kinetic model studied here is based on redox mechanism expressed by [18].

$$\text{rate} = \frac{k_1 k_2 P_{CO} P_{H_2O}}{k_1 P_{CO} + k_2 P_{H_2O}} \quad (9)$$

where P_{CO} and P_{H_2O} are the partial pressures of carbon monoxide and water, respectively. k_1 and k_2 are the model constants. After fitting the experimental data for both novel and commercial catalysts the results are presented in Table 4

The conformity of the model with the resulted kinetic experimental data at 450 oC for the novel catalyst is shown in Fig.2

Table4.
Fitting parameters of the redox-based model.

Catalyst sample	T (°C)	k_1	k_2	R^2
Novel	350	2.64×10^{-6}	∞	0.22
	400	3.06×10^{-6}	∞	0.70
	450	6.63×10^{-6}	∞	0.97
	500	1.06×10^{-5}	∞	0.55
Commercial	350	5.29×10^{-4}	100	0.95
	400	7.41×10^{-4}	∞	0.90
	450	1.11×10^{-3}	∞	0.76
	500	1.88×10^{-3}	2.57×10^{-2}	0.91

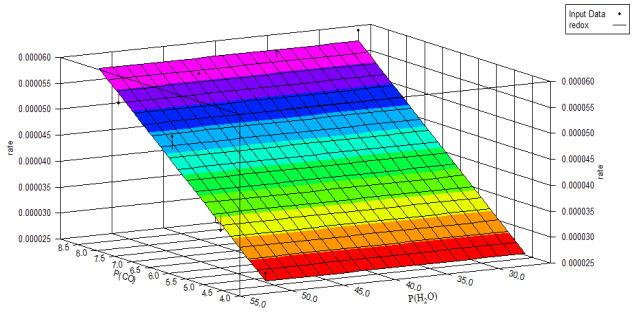

Fig. 2. The fitting of the redox-based model with the novel catalyst kinetic data in 450 °C.

Overall, it can be seen in Table 4 that the conformity of the model with the experimental data has been better for the commercial catalyst. Also it is obvious in Table 4 the extent of this fitting varies with changing temperature. Great values resulted for k_2, shown by infinitive in Table 4, implies that the reduction of H_2O to H_2 was so great that the reaction rate becomes independent from water concentration.

3.2.2. Associative mechanism

The second model was obtained from Langmuir-Hinshelwood mechanism by assuming formic acid as the intermediate represented as follows [10].

$$\text{rate} = k'' K_{CO} P_{CO} P_{(H_2O)} \left[\frac{1}{(1 + K_{CO} P_{CO} + (K_{(H_2O)} P_{(H_2O)})^{0.5}} \right]^2 \quad (10)$$

where k'' is the reaction parameter and $K_i s$ stand for the adsorption coefficients that reflect the intense of component i adsorption on the catalyst surface. The model parameters and the degree of agreement between model predictions and experimental data are listed in Table 5.

Table 5.
Fitting parameters of the associative-based model.

Catalyst sample	T (°C)	k''	K_{CO}	K_{H_2O}	R^2
Novel	350	6.23×10^{-4}	6.49	963.45	0.38
	400	3.54×10^{-2}	1.29×10^{-3}	13.80	0.70
	450	19.20	1.05×10^{-2}	30476.06	0.97
	500	1.22×10^{-2}	22.75	17729.35	0.91
Commercial	350	0.93	1.56×10^{-2}	2700.44	0.95
	400	0.80	2.55×10^{-2}	2746.59	0.89
	450	20.87	1.35×10^{-2}	25571.88	0.76
	500	9.20	1.41×10^{-2}	7333.78	0.89

Table 5 reveals that the conformity of the model with experimental data was different in various temperatures and for the commercial and novel catalysts the best fittings were observed in 450 and 350 °C, respectively. It can be seen in Table 5 that is greater than, that explains the adsorption of H_2O on the catalyst surface was so noticeable in comparison with that of CO. These large values obtained for water adsorption coefficients discover the fact that the reaction rate is not controlled by water adsorption on the catalyst surface.

The last model used for explaining the kinetic behavior of the high temperature WGSR on the catalysts is an empirical-based model expressed by [19]

$$r = k[CO]^m [H_2O]^n \quad (11)$$

Table 6.
Fitting parameters of the empirical model for the commercial catalyst.

T/K	CO			H_2O		
	m	$Ln(k[H_2O]^n)$	R^2	n	$Ln(k[CO]^m)$	R^2
623	1.032	-12.28	0.94	-0.160	-9.45	0.93
673	0.715	-11.31	0.99	-0.296	-8.59	0.99
723	1.427	-12.44	0.97	-0.657	-6.81	0.74
773	1.058	-11.13	0.99	-0.395	-7.33	0.82

After fitting the experimental data with this model the results are shown in Table 6 for the commercial catalyst and Table 7 and Fig.3 (a) and (b) for the novel one.

Table 7.
Fitting parameters of the empirical model for the novel catalyst.

T/K	CO			H_2O		
	m	$Ln(k[H_2O]^n)$	R^2	n	$Ln(k[CO]^m)$	R^2
623	1.511	-13.58	0.98	-0.470	-9.50	0.96
673	1.019	-12.63	0.94	-0.310	-8.59	0.99
723	0.943	-11.82	0.94	-0.199	-9.06	0.95
773	0.761	-10.89	0.963	-0.032	-9.25	0.95

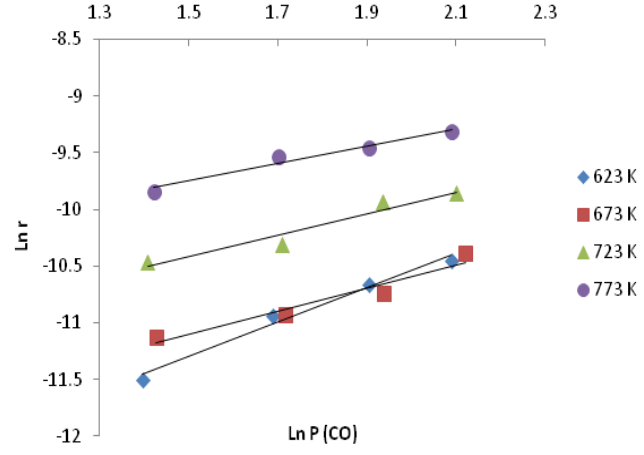

(a)

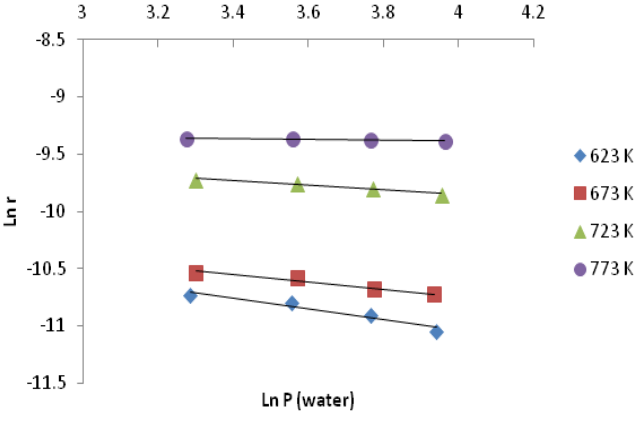

(b)

Fig. 3 (a) and (b). Fitting of the empirical model with the novel catalyst kinetic data.

The results represented in Tables 6 and 7 and also Fig.3 (a) and (b) reveal the fact that in all temperatures, the empirical model showed better coinciding with the kinetic data of the novel catalyst compared to that of the commercial one. Furthermore, the resulted values for *m* are almost around 1, which is in agreement with those reported in literature [20]. Obtaining larger numbers for the coefficients of *m* compared to that of *n,* suggesting that the reaction rate is more sensitive to the concentration of CO rather than water.

3.3.Activation energy

According to the Arrhenius expression and by considering the magnitudes of the *k* obtained by the empirical model in various temperatures, activation energy can be calculated as

$$k=k_0\, e^{-E/RT} \qquad (12)$$

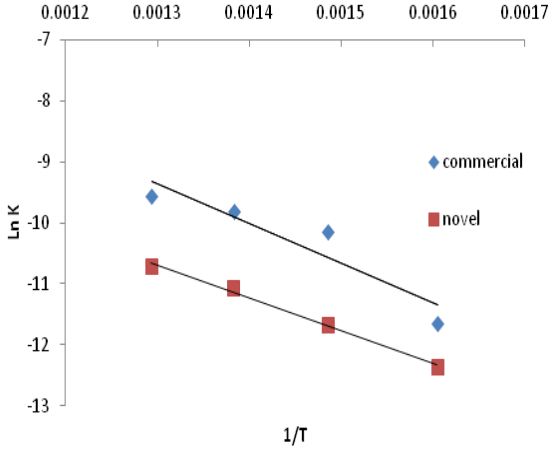

Fig. 4. Fitting the reaction coefficient obtained from the empirical data with the Arrhenius model.

Table 8.
Fitting parameters for the Arrhenius model.

Catalyst sample	E/R(K^{-1})	k_0	R^2
Commercial	6478	0.388	0.87
Novel	5393	3.673	0.99

The results of activation energy calculation for the novel and commercial catalysts are demonstrated in Table 7 and Fig. 4. In Table 8 it can be found the activation energy of the reaction catalyzed by the novel catalyst is lower than that of the one catalyzed by commercial catalyst. During the reaction, the prominent role of the catalyst is to overcome the activation energy barrier by lowering it. Therefore, the novel catalyst by causing greater reduction in the activation energy is able to facilitate the reaction more favorably compared to the commercial one.

4.Conclusions

The kinetic data for a Fe-Cr nanocatalyst and a

Fe-Cr-Cu commercial catalyst were collected by designing an experimental setup and running demanded experimentations. Modeling the kinetic data by using two redox and associative-based models as well as an empirical one revealed that the reaction rate is almost independent of water concentration reflected by obtaining large numbers for the coefficients of water reduction to hydrogen and water adsorption on the catalyst surface. With respect to the empirical model resulting greater magnitudes for m, compared to n, verified the fact that the reaction rate was more sensitive to CO concentration. Obtaining lower activation energy for the novel catalyst indicated that the novel catalyst achieved to decrease the activation energy barrier in comparison with the commercial one.

Acknowledgement

The authors express their gratitude to the IROST for financial support.

References

[1] J.S. Coleman, M. Zhang, R. M. VanNatter, C.R.F. Lund, Copper Promotion of High Temperature Shift, Catal. Today 160 (2011) 191–197.

[2] S. Shwe Hla, Y. Sun, G.J. Duffy, L.D. Morpeth, A. Ilyushechkin, A. Cousins, D.G. Roberts, J.H. Edwards, Kinetics of the water-gas shift reaction over a La0.7Ce0.2FeO3 perovskite-like catalyst using simulated coal-derived syngas at high temperature, Int. J. Hydrogen Energ. 36 (2011) 518 – 527.

[3] X.Qi, M. Flytzani-Stephanopoulos, Activity and Stability of CuCeO Catalysts in High Temperature Water Gas Shift for Fuel Cell Applications, Ind. Eng. Chem. Res.43(2004) 3055-3062.

[4] D.S. Newsome, The Water-Gas Shift Reaction, Catal. Rev. – Sci. Eng. 21 (1980) 275 – 318.

[5] B. Smith, M. Loganathan, M. S. Shantha, A Review of the Water Gas Shift Reaction Kinetics, Int. J. Chem. React. Eng. 8 (2010) 1-32.

[6] C. A. Callaghan, Doctoral Dissertation, Kinetics and Catalysis of the Water-Gas-Shift. Reaction: A Microkinetic and Graph Theoretic Approach, Worcester Polytechnic Institute (2006).

[7] S. Hilaire, X. Wang, T. Luo, R.J. Gorte, J. Wagner, A comparative study of water-gas-shift reaction over ceria-supported metallic catalysts, A comparative study of water-gas-shift reaction over ceria-supported metallic catalysts, Appl. Catal. A:Gen. 258 (2004) 271–276.

[8] C.V. Ovesen, P. Stoltze, J.K. Norskov, C.T. Campbell, A kinetic model of the water gas shift reaction, J. Catal. 134 (1992) 445–468.

[9] Q.L. Tang, Z.X. Chen, X. He, A theoretical study of the water gas shift reaction mechanism on Cu(1 1 1) model system, J. Surf. Sci. 603 (2009) 2138–2144.

[10] D.C. Grenoble, M.M. Estadt, D.F. Ollis, The chemistry and catalysis of the water gas shift reaction: 1. The kinetics over supported metal catalysts, J. Catal., 67 (1981) 90-102.

[11] A.A. Gokhale , J.A. Dumesic, M. Mavrikakis, On the mechanism of low-temperature water gas shift reaction on copper, J. Am. Chem. Soc. 130 (2008) 1402–1414.

[12] J.H. Mao, Z.M. Ni, G.X. Pan, Q. Xu, Mechanism of the copper-catalyzed water gas shift reaction, Acta Phys. Chim. Sin. 11 (2008) 2059-2064.

[13] L.C. Grabow, A.A. Gokhale, S.T. Evans, J.A. Dumesic, M. Mavrikakis, Mechanism of the water gas shift reaction on Pt: First principles, experiments, and microkinetic modeling, J. Phys. Chem. C 112 (2008) 4608–4617.

[14] J.Sun, J. DesJardins, J. Buglass, K. Liu, Noble metal water gas shift catalysis: Kinetics study and reactor design, Int. J. Hydrogen Energ. 30 (2005) 1259 – 1264.

[15] R. L. Keiski, T. Salmi, P. Niemisto, J. Ainassaari,V. J. Pohjola, A comparative study of water-gas-shift reaction over ceria-supported metallic catalysts, Appl. Catal. A:Gen 137 (1996) 349-370.

[16] I. Fishtik, R. Datta, A UBI–QEP microkinetic model for the water–gas shift reaction on Cu (111), J. Surf. Sci. 512 (2002) 229–254.

[17] A.Salehirad, S.M. Latifi, A. Miroliaee, Ion-pair complex precursor route for fabrication of high temperature shift Fe–Cr nanocatalyst, Mater. Res. Bull. 59 (2014) 104-110.

[18] Y.Li, Q.Fu, M. Flytzani-Stephanopoulos, Low-temperature water-gas shift reaction over Cu- and Ni-loaded cerium oxide catalysts, Appl. Catal., B 27 (2000) 179–191.

[19] S. Shwe Hla, D. Park, G.J. Duffy, J.H. Edwards, D.G. Roberts, A. Ilyushechkina,L.D. Morpeth, T. Nguyen, Kinetics of high-temperature water-gas shift reaction over two iron-based commercial catalysts using simulated coal-derived syngases, Chem. Eng. J. 146 (2009) 148–154.

[20] T. Bunluesin, R.J. Gorte, G.W. Graham, Studies of the water-gas-shift reaction on ceria-supported Pt, Pd, and Rh: Implications for oxygen-storage properties, Appl. Catal., B 15 (1998) 107-l 14.